Application of Thymine-based Nucleobase-modified Acrylamide as a Functional Co-monomer in Electropolymerised Thin-Film Molecularly Imprinted Polymer (MIP) for Selective Protein (Haemoglobin) Binding.

Hazim F. El-Sharif [1], Nicholas W. Turner [2], Subrayal M. Reddy [1*] and Mark V. Sullivan [2*]

* smreddy@uclan.ac.uk, mark.sullivan@dmu.ac.uk.

[1] Dr H. F. El-Sharif and Prof. S. M. Reddy, Department of Chemistry, School of Natural Sciences, University of Central Lancashire, Preston, PR1 2HE, United Kingdom.

[2] Dr N. W. Turner and Dr M. V. Sullivan, Leicester School of Pharmacy, De Montfort University, The Gateway, Leicester, LE1 9BH, United Kingdom

Abstract

Molecularly imprinted polymers (MIPs) are fast becoming alternatives to biological recognition materials, offering robustness and the ability to work in extreme environments. Here, a modified thymine-based nucleobase, with acrylamide at the 5-postion (AA-dT) was used as a co-monomer in the synthesis of a thin-film electropolymerised MIP system for the molecular recognition of the protein haemoglobin. The AA-dT co-monomer incorporated into a *N*-hydroxymethylacrylamide (NHMAm) MIP offered a two-fold superior binding affinity of the NHMAm only MIP, with K_D values of 0.72 µM and 1.67 µM, respectively. A unique AA-dT:NHMAm MIP bilayer was created in an attempt to increase the amount AA-dT incorporated into the film, and this obtained a respectable K_D value of 7.03 µM. All MIPs produced excellent selectivity for the target protein and when applied to a sensor platform (Surface Plasma Resonance), the limit of detection for the MIPs is in the nM range (3.87, 3.47, and 3.87 nM, for the NHMAm MIP, AA-dT:NHMAm MIP, and AA-dT:NHMAm MIP bilayer, respectively). The introduction of the modified thymine-based nucleobase offers a promising strategy for improving the properties of a MIP, allowing these MIPs to potentially be a highly robust and selective material for molecular recognition.

Keywords: MIP; electropolymerisation; protein; nucleobase; SPR; acrylamide; thymine

Introduction

Biosensors are analytical devices that detect the presence of biological analytes, such as biomolecules, biological structures, drug molecules, microorganisms, pesticides and toxins [1]. They convert a biological response into electrical signals, which can then be used in analytics and diagnostics [1]. The naturally occurring molecules, known as biomarkers, can be used as indicators of a biological state or condition [2, 3]. Biomarkers can be used clinically to screen, diagnose or monitor the activity of diseases, while also guiding molecular target therapy and measuring therapeutic responses [2, 3]. Protein biomarkers are especially useful in clinical diagnostics due to the range of analytical instrumentation that is available to identify and quantify proteins from complex biological samples [4]. In order to detect these biomarkers, the biosensor used usually requires a biological recognition element, such as antibodies, DNA or enzymes. These biorecognition elements bind specifically to the target molecule and ensure physicochemical signals are transduced into a measurable output [5]. While biorecognition elements can bind the target molecules with a high degree of specificity, they

do have their own issues. Along with being costly to produce, they are also sensitive to the extremes of pH and temperature, which can lead to failure within the biosensor [6, 7]. This has led to the search for new advances to replace the biological recognition elements with more robust synthetic receptors.

Molecularly imprinted polymers (MIPs) are a type of synthetic recognition molecules that are quickly becoming an established and attractive alternative to their biological counterparts. They are lost-cost, easy to produce and are robust, being resilient to the extreme temperature and pH [8]. MIPs are synthetic materials that are prepared by the copolymerisation of functional and cross-linking monomers, in the presence of a template [9, 10]. Using a self-assembly approach, suitable functional monomers are pre-organised around a template molecule, forming a complex by virtue of hydrogen-bonding. The monomers are polymerised with a suitable cross-linker, preserving the complexes within the polymer matrix. Subsequent removal of the template from the polymer matrix leaves molecular cavities that are complementary in size, shape and orientation to the template. These cavities are then capable of selectively binding the target analyte molecules [11, 12].

Traditionally, MIPs were usually prepared using free radical polymerisation, which resulted in a bulk monolith. In order to remove the template and access the recognition cavities, the monolith needed to be processed, which is achieved though grinding and sieving and forms micron sized particles. This process is extremely laborious and can potentially damage the binding sites, resulting in a loss of binding affinity [13]. Nanoparticle-based MIPs (NanoMIPs) have been developed in order to combat that loss of affinity. The nanoMIPs are typically grown on the template to approximately 100-150 nm in size, leaving the template imprinted upon the surface [14, 15]. This means that the requirement of breaking-up the polymer, in order to gain access to allow the removal of the template is not necessary, thus leaving a greater proportion of the binding sites retained. Along with an increased surface particle, this results in increased binding affinity for the nanoMIPs. However, the reported yields for nanoMIPs can be potentially low [16, 17].

Thin-film MIPs are an alternative to bulk (3D) MIPs and nanoMIPs, that have shown potential to be used as a recognition element within a biosensor [18]. These are usually produced be either stamping or spin-coating a polymerising solution onto a solid surface [18], or by using electrochemical methods for the polymerisation [19]. In a thin-film, the template binding sites are located on the exposed film surface and the films can be easily integrated onto a sensor surface [20]. They are vital to the transduction of a signal used within sensing platforms, including surface plasma resonance SPR [21]. Free-standing and transferrable thin-sheets (thicknesses greater than 200 µm) have been produced and have advantages of being movable and less fragile than a thin-film [13]. It is difficult to control the thicknesses of these sheets and they could potentially be too thick and could reduce the signal strength [13]. Electropolymerisation can be an advantageous technique as it allows for the thickness of the polymer to be controlled, and with a wide range of electroactive monomers to choose from, the films can be easily attached to a sensor surface of any shape or size [22]. Furthermore, the use of an initiator, UV light or heat is not needed for the electropolymerisation of a MIP onto a transducer surface. Instead the MIP-film is deposited, from functional monomer solution (sometimes containing an appropriate cross-linker) of a porogenic solvent, directly onto the surface, in the presence of a template [23, 24]. The film thickness is controlled by the amount of charge transferred during the electropolymerisation, with surface morphology controlled by the selection of a suitable solvent and supporting electrolyte [25, 26]. Over oxidisation is an issue that can occur with electroactive monomers, particular at lower potentials, in an oxygen or water containing environment, and can cause an increase the thickness of the film ultimately leading to a loss in conductivity [27-30]. While, the loss in conductivity is a disadvantage, a wide range of bioanalytical applications have resulted from the incorporation of imprinted, overoxidised monomer layers, into sensor platforms [31-33].

Acrylamide-based compounds have shown promise for their use as functional monomers for protein-based imprinting. These monomers are chosen as they can contain a range of functional groups (OH, C=O, NH_2, etc.) that are able to optimise hydrogen-bonding effects to maximise binding association in a template-monomer complex [10, 34]. Acrylamide-based monomers also increases the chance of the monomer being water-soluble and this is important for protein imprinting, as using water as a polymerisation solvent could avoid any potential denaturation and changes to the conformation of the protein structure, that could happen if an organic solvent were to be used. While acrylamide-based MIPs show continued promise, they can still suffer from low affinity and specificity [13]. Successful incorporation of DNA aptamers and fragments as functional monomers has been achieved. These aptamer-MIP (aptaMIP) hybrids have shown that using the polymer scaffold to stabilise the aptamer can offer improved binding affinities [15, 35]. However, the aptamers do need to be specifically designed to suit the template, meaning the resulting aptaMIP synthesis can be quite complex at times. An alternative could be to use a DNA nucleobase (such as thymine), modified with a polymerisable functional group, as the functional monomer and to potentially allow for DNA type recognition (due to enhanced hydrogen bonding interactions between functional monomer and template), but with the simplicity of a standard MIP synthesis.

Here we present, for the first time, the use of a modified DNA nucleotide acrylamide dT as a functional monomer in the electropolymerisation of an acrylamide-based hydrogel thin-film MIP (eMIP) for the target protein, haemoglobin. Using an electropolymerisation technique, three monomers (a modified acrylamide, acrylamide dT and a mixture of the two), were polymerised on the gold surface of a SPR chip. After removal of the template, different concentrations of the target molecule, bovine haemoglobin (BHb), was injected over the thin-films, in order to calculate the dissociation constants (K_D) of the MIPs. The non-target proteins, bovine serum albumin (BSA) and trypsin, both also found in blood samples, were also injected over the thin-films, as control proteins, in order to show MIP recognition and specificity for the protein target.

Materials and Methods

Materials

Plain gold (Au) Surface Sensor chips were purchased from Reichert Technologies Life Sciences, Buffalo, New York, USA.

Celite®, chloroform, dimethylsulfoxide (DMSO), dipotassium phosphate, dimethylformamide (DMF), ethanolamine, *N*-(3-dimethylaminopropyl)-*N*'ethylcarbodiimide (EDC), *N*-Hydroxysuccinimide (NHS), palladium acetate, potassium chloride (KCl), sodium chloride, Tween 20, and tributylamine were all purchased and used without purification from Fisher Scientific UK Ltd, Loughborough, UK.

Bovine haemoglobin (BHb), bovine serum albumin (BSA), *N*-hydroxymethylacrylamide (NHMAm, 48% w/v), *N,N'*-methylenebisacrylamide (MBAm), phosphate buffered saline tablets (PBS, 10 mM, pH 7.4±0.2), potassium ferricyanide ($K_3[Fe(CN)_6]$), potassium peroxydisulfate (KPS), sodium nitrate ($NaNO_3$), and trypsin were all purchased and used without purification from Merck Life Science UK Ltd, Dorset, UK.

5-Iodo-2'-deoxyuridine was purchased from LGC LINK (Bellshill, Lanarkshire, Scotland).

Buffers were prepared in ultra-pure water (UPW, 18.2 MΩ cm^{-1}) and filter sterilised (0.2 μm).

Methods

Synthesis of Acrylamide-dT

Partially following the synthesis of Allabush et al. [36], 5-Iodo-2'-deoxyuridine (1.00 g, 2.82 mmol) and palladium acetate (60 mg, 0.28 mmol) were dissolved in DMF (3 mL) in a 10 mL microwave vial, equipped with a small magnetic stirrer bar. Tributylamine (0.67 mL, 2.82 mmol) and *N,N'*-methylenebisacrylamide (1.09 g, 7.06 mmol), were then added. The solution was vortexed for 30 seconds, followed by stirring and degassing with nitrogen for 10 minutes. The vial was then tightly sealed, and the mixture irradiated in a microwave for 10 minutes at 100 °C. After irradiation, the reaction was cooled to room temperature before the reaction mixture was filtered through Celite®. The product was then isolated by precipitation from cold chloroform, to yield an off white solid (703 mg, 66 %). NMR analysis carried out using Jeol ECZ 600 MHz, giving a ^{1}H NMR (600 MHz, $(CD_3)_2SO$) δ 11.56 (s, 1H), 8.69 (t, J=5.9 Hz, 2H), 8.32 (s, 1H), 7.18 (d, J = 15.6 Hz, 1H), 6.96 (d, J ¼ 15.6 Hz, 1H), 6.30–6.21 (m, 1H), 6.16–6.09 (m, 2H), 5.64–5.58 (m, 1H), 5.27 d, J ¼ 4.3 Hz, 1H), 5.16 (t, J ¼ 5.0 Hz, 1H), 4.54 (t, J ¼ 5.8 Hz, 2H), 4.29–4.23 (m, 1H), 3.82–3.78 (m, 1H), 3.70–3.55 (m, 1H), 2.18–2.13 (m, 2H). IR neat (cm^{-1}): 3295 (m, OH/NH), 3065 (w, CH), 1689 (s, C=O), 1650 (s, C=C).

Electrochemical deposition of layer

Thin-film hydrogel layers were fabricated directly onto Au-SPR chip surfaces by electrochemical polymerisation using cyclic voltammetry (CV). The potential was cycled between −0.2 V and −1.4 V for 10 cycles at 50 mV s^{-1} (~ 8 min, RT, 22±2 °C). Each SPR chip experiment comprised the following e-polymerisation formula:

1 - PBS containing 186 µM BHb protein template, 0.76 M NHMA as the functional monomer, 38.92 mM MBAm as the cross-linker, 0.29 M $NaNO_3$, and 48.15 mM KPS. This is known as **NHMAm eMIP**

2 **-** PBS containing 186 µM BHb, 0.76 M NHMA and 16 mM AA-dT (dissolved in DMSO) as the functional monomers, 38.92 mM MBAm, 0.29 M $NaNO_3$, and 48.15 mM KPS. To create an eMIP with the monomer NHMAm:AA-dT ratio of 47.5:1. This is known as **NHMAm:AA-dT eMIP .**

3 **-** first layer: PBS containing 0.76 M NHMA and 160 mM AA-dT (dissolved in DMSO) as the functional monomers, 38.92 mM MBAm, 0.29 M $NaNO_3$, and 48.15 mM KPS. Second Layer: PBS containing 186 µM BHb protein template, 0.76 M NHMA as the functional monomer, 38.92 mM MBAm as the cross-linker, 0.29 M $NaNO_3$, and 48.15 mM KPS. To create an eMIP bilayer with the monomer NHMAm:AA-dT ratio of 4.75:1 This is known as **NHMAm:AA-dT eMIP bilayer.**

Au-SPR polymer deposition was then characterised via typical CV scans (50 mV s^{-1}), in triplicate of an external 5 mM potassium ferricyanide solution containing 0.5 M KCl as supporting electrolyte. All electrochemical measurements were performed using an EQCM three-electrode single-compartment cell (ALS, Japan) comprising an exposed area of the Au-SPR chip (~5 mm^2) as the working electrode (WE), a Ag/AgCl reference electrode (3M NaCl) and a platinum counter electrode powered by an Autolab PGSTAT204 potentiostat and NOVA2.1.4 software.

Removal of Template Molecule Using SPR

Previous work, showed the efficient removal of a target molecule from a nanoMIP immobilised onto an Au surface, using a regeneration buffer of 10 mM Glycine-HCl at pH 2 [15, 35]. This was adapted for the removal of the protein template to be assessed by monitoring using the Reichert 2SPR. From a running buffer of PBST (PBS with 0.01 % v/v Tween 20 added), template removal was initiated by the injection of 100 µL of the regenerating buffer (10 mM Glycine-HCl, pH 2) for 1 minute (template removal) followed by PBST for 2 minutes (template dissociation). This was repeat five times to allow all surface imprinted template molecules to be completely removed.

Kinetic Analysis Using SPR

Adapted from Sullivan et al. [15, 35], kinetic analysis was initiated by the injection of the running buffer, PBST (blank) onto the MIP immobilised onto the gold chip surface, for 2 minutes, followed by PBST for 5 minutes. The binding kinetics of an individual MIP to the selected target protein (BHb) was determined from serial dilutions (five concentrations, 4 - 64 nM). Each dilution was injected for 2 minutes (for target association) followed by PBST for 5 minutes (for target dissociation). After the dissociation, the target protein was removed from the MIP surface by an injection of a regenerating buffer (10 mM Glycine-HCl, pH 2) for 1 minute, followed by PBST or 1 minute. The same procedure was repeated for the remaining four dilutions of the protein. This process was repeated with a blank Au chip (without MIP immobilised) as a control; this was subsequently subtracted from signal for their respective rebinding MIP studies. Selectivity for the MIPs was investigated by repeating the SPR kinetic analysis, but with two non-target proteins (BSA and Trypsin) at the same concentrations, instead. All analyses were carried out at 25 °C.

The SPR responses from the five concentrations of the target protein were fitted to a 1:1 bio-interaction model (Langmuir fit model) utilising TraceDrawer Software. Association rate constant (k_a), dissociation rate constant (k_d), and maximum binding (B_{max}) were fitted globally, whereas the BI signal was fitted locally. The equilibrium dissociation constant (K_D) was calculated from the ratio k_d/k_a. A SPR sensorgram calibration was created using a concentration range of 4-64 nM and was used to calculate a theoretical LOD.

Results and Discussion

Synthesis of Acrylamide-dT

Partially following the method of Allabush et al. the synthesis of the target Acrylamide-dT involved using the commercially available 5-iodo-2'deoxyuridine and substituting the iodine at C5 with an acrylamide group *via* the Heck reaction with *N,N'*-methylenebisacrylamide (Figure 1) [36]. A microwave-assisted procedure was used, which was adapted from Fujimoto and allowed the two entities to be coupled together to form Acrylamide-dT in a good yield (75%) [37]. *N,N'*-methylenebisacrylamide was used in excess in order to minimise coupling of 5-iodo-2'-deoxyuridine to both sides of the molecule. The product was precipitated from cold chloroform, and washed with cold chloroform to remove the excess *N,N'*-methylenebisacrylamide.

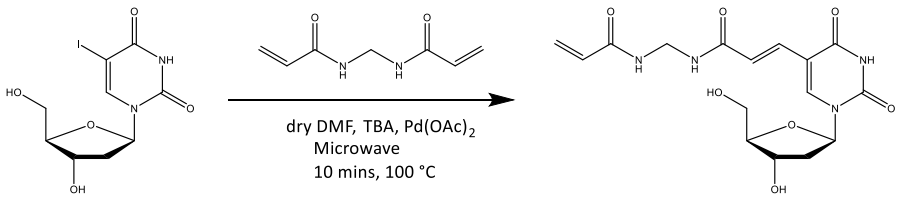

Figure 1. The synthesis of Acrylamide-dT.

Electrochemical MIP Fabrication

For each chip modification, thin-film hydrogel layers were fabricated directly onto the Au surface of the SPR chip, using electrochemical polymerisation *via* cyclic voltammetry, with the voltammograms shown in Figure 2. In the work of Sullivan et al. the functional monomer NHMAm was shown to be an excellent choice for hydrogel-based MIPs in the imprinting of protein targets [10, 13], with computational studies suggesting that this was due to a high number of helical side-chain interactions and minimal backbone disturbances [10]. Therefore, NHMAm was used as the main functional

monomer for these electropolymerised thin-film hydrogel MIPs (eMIPs). While it would have been preferable for the modified nucleobase, Acrylamide-dT (AA-dT), to be water soluble, this proved not to be the case. This resulted in the use of an organic solvent (DMSO) was needed to dissolve the monomer. This had the potential to cause issues, as the use of a high concentration of organic solvent has been shown to denature protein template molecules at the pre-polymerisation stage [38], resulting in MIP cavities that do not correspond to the target molecule, hence a poorer performing MIP. This resulted in the exploration of two different methods for the incorporation of AA-dT in the fabrication of the MIP. The first method involved dissolving 16 mM of AA-dT in a minimal amount of DMSO, before being dissolved into the polymerisation solution, allowing AA-dT to be used as co-monomer. The second method involved firstly polymerising AA-dT on to the Au surface, effectively functionalising the chip with AA-dT. Next, the polymerisation solution containing NHMAm (as the functional monomer) and template was added, to create an AA-dT:NHMAm eMIP bilayer. This method allowed for the increase (10 fold) of the amount of AA-dT that could be incorporated into the MIP.

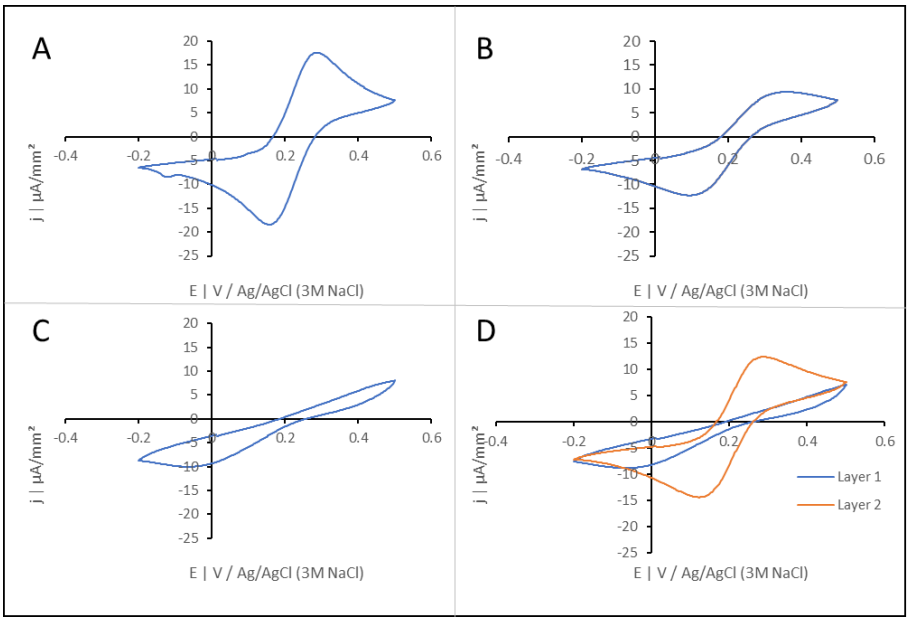

Figure 2. Cyclic voltammograms of $K_3[Fe(CN)_6]$ (5mM in 0.5 M KCl) on: (A) Bare SPR chip, (B) NHMAm eMIP layer, (C) NHMAm:AA-dT eMIP layer, and (D) NHMAm:AA-dT eMIP bilayer.

Figure 2A shows the voltammogram of the bare gold surface, showing the traditional shape of the reversible reduction of the ferricyanide ion ($[Fe(CN)_6^{3-}]$) [39]. Figure 2B shows the expected corresponding diminution in both anodic and cathodic peak currents of the ferro/ferricyanide redox couple following electrodeposition of the NHMAm eMIP on the Au-chip surface. The addition of the AA-dT as a functional monomer, to create the NHMAm:AA-dT eMIP, seems to have the largest diminutive effect on the ferro/ferricyanide redox peaks, as shown in Figure 2C. To maximise the amount of AA-dT, a different approach was adopted to create an eMIP bilayer. As can be seen in Figure 2D, the layer of AA-dT (layer 1) was deposited onto the surface, diminishing the ferricyanide peak. Upon addition of the NHMAm eMIP layer (Figure 2D, layer 2), the ferricyanide peak is now less diminished (compared with Figure 2B), which not only suggests that the AA-dT first layer has been

damaged in the process of adding of the NHMAm second layer, but also less NHMAm has been added compared with Figure 2B.

Removal of Template Molecule Using SPR

With the thin-film deposited on to the Au surface of the SPR chip, the template molecule needed to be removed to allow for the MIP cavities to be exposed for rebinding. Previous work by Sullivan et al. used a regeneration buffer of 10 mM Glycine-HCl at pH 2, to remove the target molecule from MIP nanoparticles (nanoMIPs) and Aptamer-MIP hybrid nanoparticles (AptaMIPs), immobilised onto the Au chip surface [15, 35]. This allowed for the chip to be used multiple times for the SPR kinetic studies for the determination of dissociation constant of the nanoMIPs and aptaMIPs. Adapting this approach here, allowed for the removal of the template to be assessed by monitoring using SPR as shown in Figure S2, with Figure S2A, S2B, and S2C corresponding to the NHMAm eMIP, NHMAm:AA-dT eMIP and NHMAm:AA-dT eMIP bilayer, respectively. As seen in Figure S2 there is a large initial drop in signal, caused by a change in the refractive index of the buffer solution. The baseline then returns, but at a lower level, thus indicating removal of the template. This was repeated five times, until the baseline indicated maximum removal (Wash 5) and was achieved with all three (NHMAm eMIP, NHMAm:AA-dT eMIP and NHMAm:AA-dT eMIP bilayer) thin-film eMIPs shown in Figure S2A, S2B, and S2C, respectively. No visible deterioration in the layers were observed, nor a drop in SPR baseline signal (corresponding to thickness of deposited layer); or loss of electrochemical signal was observed. This suggests that all layers formed were stable under experimental conditions.

Kinetic Analysis Using SPR

The SPR sensorgrams in Figure 3 show the interactions of the target protein (haemoglobin) at five different concentrations captured by the NHMAm eMIP (Figure 3A), NHMAm:AA-dT eMIP (Figure 3B), NHMAm:AA-dT eMIP bilayer (Figure 3C), electropolymerised on the sensor surface. Tween 20 (0.01 % v/v) was added to the running buffer in order to reduce non-specific binding.

To study cross-reactivity and non-specific binding, non-target proteins (BSA and trypsin) were also investigated. The binding of BSA is shown in Figure 3D (NHMAm eMIP), Figure 3E (NHMAm:AA-dT eMIP) and Figure 3F (NHMAm:AA-dT eMIP bilayer) and the binding of trypsin is shown in Figure 3G (NHMAm eMIP), Figure 3H (NHMAm:AA-dT eMIP) and Figure 3I (NHMAm:AA-dT eMIP bilayer). The experiments were repeated in triplicate and the SPR curves were fitted to a 1:1 interaction model. The overall equilibrium dissociation constant (K_D) of NHMAm eMIP, NHMAm:AA-dT eMIP and NHMAm:AA-dT bilayer towards the target and non-target proteins were determined and summarised in Table 1.

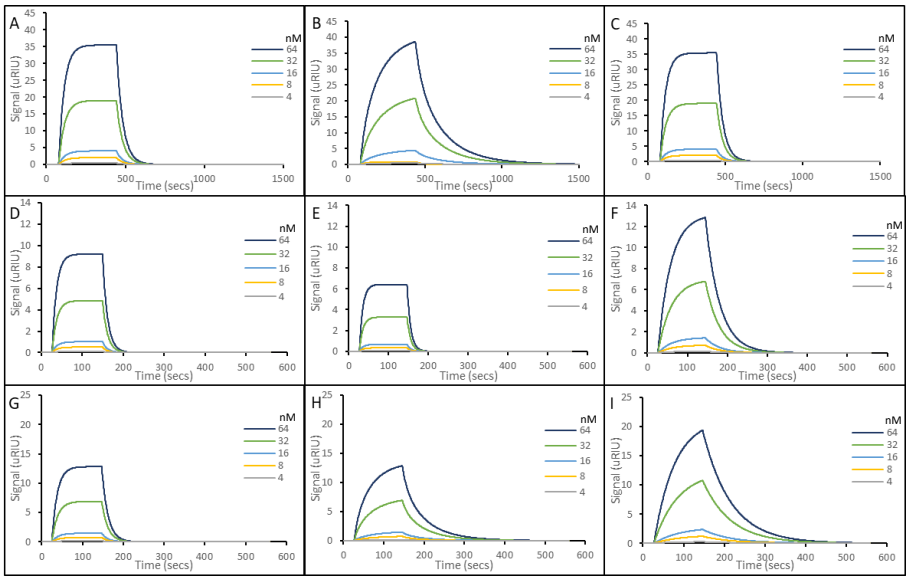

Figure 3. Representative SPR sensorgrams of molecular interactions of various hydrogel thin-film MIPs, electropolymerised onto Au chips, to solutions containing five concentrations of target and non-target proteins, between 4 and 64 nM. **(A)** BHb binding to BHb-imprinted NHMAm eMIP; **(B)** BHb binding to BHb-imprinted NHMAm:AA-dT eMIP; **(C)** BHb binding to BHb-imprinted NHMAm:AA-dT eMIP bilayer; **(D)** BSA binding to BHb-imprinted NHMAm eMIP; **(E)** BSA binding to BHb-imprinted NHMAm:AA-dT eMIP; **(F)** BSA binding to BHb-imprinted NHMAm:AA-dT eMIP bilayer; **(G)** Trypsin binding to BHb-imprinted NHMAm eMIP; **(H)** Trypsin binding to BHb-imprinted NHMAm:AA-dT eMIP; **(I)** Trypsin binding to BHb-imprinted NHMAm:AA-dT eMIP bilayer.

Table 1. Calculated equilibrium dissociation constant (K_D) of the imprinted materials.
[ab]**Imprinted polymer layer**

	K_D (M)		
	BHb	**BSA**	**Trypsin**
NHMAm	16.7×10^{-7} ($\pm 1.3 \times 10^{-7}$)	4.76×10^{-3} ($\pm 0.4 \times 10^{-3}$)	1.87×10^{-3} ($\pm 0.6 \times 10^{-3}$)
NHMAm:AA-dT	7.15×10^{-7} ($\pm 0.6 \times 10^{-7}$)	4.83×10^{-3} ($\pm 0.7 \times 10^{-3}$)	1.46×10^{-3} ($\pm 0.8 \times 10^{-3}$)
NHMAm:AA-dT bilayer	70.3×10^{-7} ($\pm 5.8 \times 10^{-7}$)	4.03×10^{-3} ($\pm 0.6 \times 10^{-3}$)	0.92×10^{-3} ($\pm 0.1 \times 10^{-3}$)

[a] All experiments performed under ambient conditions.
[b] Number of repeats = 3.

The K_D of the interaction between haemoglobin and the haemoglobin specific MIPs have been calculated as 1.67 (±0.13) x 10^{-6} M, 0.715 (±0.06) x 10^{-6} M and 7.03 (±0.58) x 10^{-6} M (Table 1) for NHMAm eMIP, NHMAm:AA-dT MIP, and NHMAm:AA-dT eMIP bilayer, respectively. The addition of AA-dT as co-monomer improves the K_D approximately two-fold (0.715 *vs* 1.67 x 10^{-6} M), compare with NHMAm eMIP, made in the absence of the polymerisable DNA base. This clearly shows that the addition of the AA-dT as functional co-monomer improves performance. The ratio ($K_{D\ \text{NHMAm:AA-dT eMIP}}$/

$K_{D\ NHMAm\ eMIP}$) of relative signal strengths (Figure 3) show a ratio of 2.3, which suggests that the NHMAm:AA-dT eMIP binds more protein, at a given concentration, and support it having greater affinity.

The NHMAm:AA-dT eMIP bilayer has the lowest K_D, approximately four-fold (1.67 *vs* 7.3 x 10^{-6} M) decrease, compared with NHMAm eMIP. These shows that creating sequential polymer layers of each monomer has a negative impact on performance (Figure 3/ Table 1). In the bilayer system, a non-imprinted AA-dT was deposited first followed by a second imprinted layer of just NHMAm. The idea here was to pre-concentrate the AA-dT onto the surface before imprinting. The reduction in performance highlights the importance of templation using the specific monomer AA-dT rather than just its presence. Figure 2D also shows that the deposition of the second layer was not as successful, which also will affect performance compared to the NHMAm layer only. In summary, the data supports the use of the AA-dT monomer as a core component rather than just it's close proximity, even in excess.

Overall, the K_D value (1.67 x 10^{-6} M) of the NHMAm-based eMIP is comparable with those reported in literature, the work of Moreira et al., produced an electropolymerised acrylamide thin-film eMIP with K_D value of 3 x 10^{-6} M [40, 41]. The approximate two-fold increase is to be expected, with the work of Sullivan et al. showing that the NHMAm functional monomer has improved binding compared with acrylamide, in protein binding [10, 13]. The addition of the modified nucleobase (AA-dT) as a functional monomer increases the affinity by over two-fold compared with the NHMAm eMIP and increases nearly 10-fold compared with existing technology [40, 41]. This shows that the addition of the polymerisable DNA base, AA-dT, as a co-monomer has a positive effect and has increased the efficiency of the MIP, notably since the K_D values of eMIPs have been reported in other works are in the low mM range [42, 43].

The use of a non-imprinted polymer (NIP) as a control to generate an imprinting factor (IF – ratio of MIP binding vs NIP binding) is one method traditionally used to measure of the strength of interaction between functional monomer and target molecule [13], however we have elected to not do this. It has been shown in multiple studies that a NIP has significantly different morphology and behaviour to an imprinted layer, and this is exacerbated in protein imprinting due to the relative size of template and "binding pocket". This decision is further supported by the understanding that in studies where monomer selection is considered, it has been demonstrated that effectiveness of binding a target to a NIP should only be used to inform us of monomers to investigate for MIP development to enhance such innate binding properties. Since we know acrylamide polymers have already shown to have affinity for protein by NIP and to a greater extent by MIP, there is no further need to demonstrate a NIP effect. Given our aim is to develop a sensor platform, and we demonstrate selectivity against other protein targets the NIP is not required.

As such, it has now become generally accepted that the use of a selectivity factor (SF – ratio of target binding/non-target binding) is generally considered more favourable and a better measure of the binding ability of the MIP [44-46]. The recent development of MIP nanoparticles (NanoMIPs), using a solid phase synthesis method, require a nucleation site, via an affixed template molecule meaning by definition (a NIP is produced in the absence of the template) it is impossible to create a NIP nanoparticle [16, 17, 47]. Thus, making the IF value and subsequently the NIP redundant. Instead, to evaluate the ability of the thin-film MIPs to discriminate between BHb and other proteins, all three MIPs were challenged with the non-target proteins, BSA and trypsin, chosen as they are representative proteins that may be found in the same matrix that BHb can be found. SPR analysis, shown in Figures 3D – 3I revealed that while there is some binding of the non-target proteins (BSA and trypsin) to the materials, the affinity (shown in Table 1) is vastly reduced (K_D values of 4.76 (±0.4) mM, 4.83 (±0.7)

Commented [NT1]: https://onlinelibrary.wiley.com/doi/10.1002/jmr.2855

Commented [NT2]: https://pubs.acs.org/doi/10.1021/ja205632t
https://doi.org/10.1016/j.biomaterials.2014.05.079
https://doi.org/10.1016/j.actbio.2015.09.012
https://doi.org/10.3390/polym10010097

Commented [NT3]: https://pubs.acs.org/doi/10.1021/acs.jpcb.9b03091

mM, 4.03 (±0.6) mM, 1.87 (±0.6) mM, 1.46 (±0.8) mM, and 0.92 (±0.1) mM, respectively). The K_D values presented in Table 1, show a 10 000-fold increase in affinity of the MIP towards the target protein compared with the non-target proteins. This demonstrates that all three eMIP systems studied, as expected, are selective for the haemoglobin target only. The K_D values between MIPs are similar, and the decrease observed is also similar, further suggesting that any binding of BSA or trypsin to the thin-films is non-specific [15, 35]. The observed relative signal is comparable as well, suggesting there is no differences in affinity. In summary, the NHMAm:AA-dT eMIP bilayer has less affinity for the target molecule, but higher cross-reactivity when compared to the other thin-film MIPs, suggesting they (NHMAm and NHMAm:AA-dT eMIPs) are superior materials.

All three eMIPs where investigated for the determination of the theoretical lower limit of detection (LOD) for BHb using the SPR system. By using the maximum signal (µRIU) from the fitted SPR curves (Figure 3), concentration calibrations were plotted and shown in Figure 4. This allowed for the estimation of the theoretical lower LOD. All three MIPs produced similar theoretic LODs with 3.87 nM, 3.41 nM, and 3.87 nM, for NHMAm eMIP (Figure 4A), NHMAm:AA-dT eMIP (Figure 4B), and NHMAm:AA-dT eMIP bilayer (Figure 4C), respectively. The estimates show that the lower LODs are consistent across the MIPs and are similar to the lowest observable SPR signal (4 nM). These LODs are both acceptable and superior to other thin-films MIPs used to detect haemoglobin by SPR. For example, the work by Wang et al. produced a 3-aminophenylboronic acid (3-APBA) thin-film eMIP for the detection of haemoglobin, with a lower LOD of 6.80 nM [48]; the LOD from the NHMAm:AA-dT eMIP is approximately two-fold lower. This suggests that the LOD and observed linearity are within a practical application range for the detection of protein in biological samples.

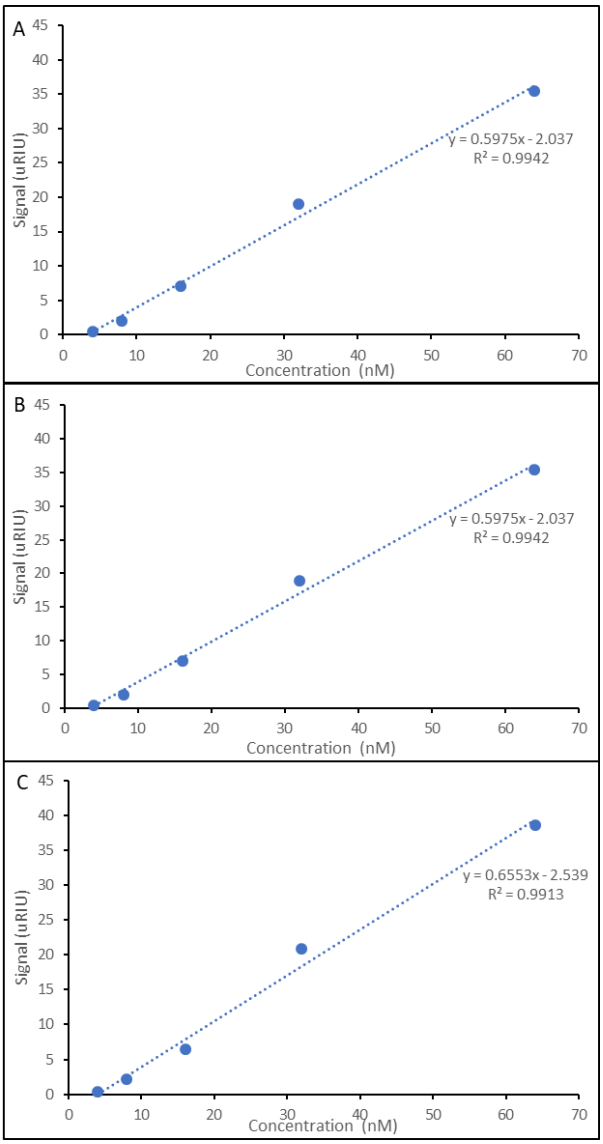

Figure 4. Elucidation of limit of detection of SPR sensor. Relative signal vs concentration **(A)** BHb binding to BHb-imprinted NHMAm eMIP; **(B)** BHb binding to BHb-imprinted NHMAm:AA-dT eMIP; **(C)** BHb binding to BHb-imprinted NHMAm:AA-dT eMIP bilayer.

Overall, the data presented here supports that the inclusion of a polymerisable DNA base (AA-dT) as a co-monomer is beneficial and significantly improves the affinity and specificity of the electropolymerised MIP. While the differences in affinity data may appear small, in analytical terms

the doubling of performance is significant and could potentially be the difference between a positive and negative result.

Conclusion

Here we have developed a simple and effective thin-film MIP that is capable of selectively binding the target protein haemoglobin. By incorporating a polymerisable DNA base (AA-dT) as a co-monomer, we are able to improve the performance of the material, which is observed in terms of the affinity of the material. The synthesis of these materials is relatively straight forward, using an existing microwave method, AA-dT can be synthesised quickly and in high yields. Then, using an electro-polymerisation methodology, the AA-dT can be incorporated as a co-monomer within the eMIP. The gentle conditions of the technique result in the protein template molecules to retaining their stability, allowing for the creation of selective cavities within the MIP thin-film. The method allows for the creation of highly selective thin-films, which, as demonstrated, can be easily incorporated on to the surface of a gold chip and could potentially lead the way for potential sensor applications. Multiple opportunities for improvements exist, with a variety of potential targets as well as alterations to the chemistry and the potential to incorporate different DNA bases as co-monomers, especially given the well-understood hydrogen-bonding capabilities of nucleic acid bases. Possible changes to the running buffer (increasing the surfactant concentration) or longer equilibrium times could further reduce cross-reactivity. While questions, currently under investigation, may remain over the practical use of these materials in sensor applications, these materials, as demonstrated, have the potential to offer nM LODs and combined with their robust polymeric nature, result in a highly effective biorecognition materials for biosensors.

Acknowledgements

MS and NT wish to thank the EPSRC for financial support (EP/S003339/1). HE and SM wish to thank the University of Lancashire for financial support.

[1] N. Bhalla, P. Jolly, N. Formisano, P. Estrela, Introduction to Biosensors, Essays in Biochemistry. 60 (2016) 1-8.

[2] K. Strimbu, J.A. Tavel, What are biomarkers?, Current Opinion in HIV & AIDS. 5 (2010) 463-466.

[3] S. Dietze, A. Patzak, Biomarkers, Acta Physiologica. 216 (2016) 379-382.

[4] R. Mayeux, Biomarkers: Potential Uses and Limitations, NeuroRx. 1 (2004) 182-188.

[5] H. Mischak, G. Allmaier, R. Apweiler, T. Attwood, M. Baumann, A. Benigni, S.E. Bennett, R. Biscoff, E. Bongcam-Rudloff, G. Capasso, J.J. coon, P. D'Haese, A.F. Dominiczak, M. Dakna, H. Dihazi, J.H. Ehrich, -. Fernandez P., D. Fliser, J. Frokiaer, J. Garin, M. Girolami, W.S. Hancock, M. Haubitz, D. Hochstrasser, R.R. Holman, J.P.A. Ioannidis, J. Jankowski, B.A. Julian, J.B. Klein, W. Kolch, T. Luider, Z. Massy, W.B. Mattes, F. Molina, B. Monsarrat, J. Novak, K. Peter, P. Rossing, M. Sánchez-Carbayo, J.P. Schanstra, O.J. Semmes, G. Spasovski, D. Theodorescu, V. Thongboonkerd, R. Vanholder, T.D. Veenstra, E. Weissinger, T. Yamamoto, Recommendations for biomarker identification and qualification in clinical proteomics, Science Translational Medicine. 2 (2010) 46ps42.

[6] A. Gray, A.R.M. Bradbury, A. Knappik, A. Plückthun, C.A.K. Borrebaeck, S. Dübel, Animal-free Alternatives and the Antibody Iceberg, Nature Biotechnology. 38 (2020) 1234-1239.

[7] M.V. Sullivan, W.J. Stockburn, P.C. Hawes, T. Mercer, S. Reddy M., Green synthesis as a simple and rapid route to protein modified magnetic nanoparticles for use in the development of a fluorometric molecularly imprinted polymer-based assay for detection of myoglobin, Nanotechnology. 32 (2021) 095502.

[8] K. Mosbach, O. Ramstron, The Emerging Technique of Molecular Imprinting and its Future Impact on Biotechnology., Nature Biotechnology. 14 (1996) 163-170.

[9] E.V. Piletska, A. Guerreiro, M.J. Whitcombe, S.A. Piletsky, Influence of the Polymerization Conditions on the Performance of Molecularly Imprinted Polymers., Macromolecules. 42 (2009) 4921-4928.

[10] M.V. Sullivan, S.R. Dennison, G. Archontis, J.M. Hayes, S.M. Reddy, Towards Rational Design of Selective Molecularly Imprinted Polymers (MIPs) for Proteins: Computational and Experimental Studies of Acrylamide Based Polymers for Myoglobin., The Journal of Physical Chemistry B. 123 (2019) 5432-5443.

[11] T. Muhammad, Z. Nur, E.V. Piletska, O. Yimit, S.A. Piletsky, Rational Design of Molecularly Imprinted Polymer: The Choice of Cross-linker, Analyst. 137 (2012) 2623-2628.

[12] D. Refaat, M.G. Aggour, A.A. Farghali, R. Mahajan, J.G. Wiklander, I.A. Nicholls, S.A. Piletsky, Strategies for Molecular Imprinting and the Evolution of MIP Nanoparticles as Plastic Antibodies—Synthesis and Applications, International Journal of Molecular Sciences. 20 (2019) 6304.

[13] M.V. Sullivan, S.R. Dennison, J.M. Hayes, S.M. Reddy, Evaluation of Acrylamide-based Molecularly Imprinted Polymer Thin-Sheets for Specific Protein Capture - a Myoglobin Model, Biomedical Physics & Engineering Express (2021) 045025.

[14] F. Canfarotta, S.A. Piletsky, N.W. Turner, Generation of High-Affinity Molecularly Imprinted Nanoparticles for Protein Recognition via a Solid-Phase Synthesis Protocol, Methods in Molecular Biology. 2073 (2020) 183-194.

[15] M.V. Sullivan, F. Allabush, D. Bunka, A. Tolley, P.M. Mendes, J.H.R. Tucker, N.W. Turner, Hybrid aptamer-molecularly imprinted polymer (AptaMIP) nanoparticles selective for the antibiotic moxifloxacin, Polymer Chemistry. 12 (2021) 4405.

[16] A. Poma, A.P. Turner, S.A. Piletsky, Advances in the Manufacture of MIP nanoparticles. , Trends in Biotechnology. 28 (2010) 629-637.

[17] F. Canfarotta, A. Poma, A. Guerreiro, S.A. Piletsky, Solid-Phase Synthesis of Molecularly Imprinted Nanoparticles., Nature Protocols. 11 (2016) 443-455.

[18] G. Erturk, B. Mattiasson, Molecular Imprinting Techniques Used for the Preparation of Biosensors., Sensors. 17 (2017) 288.

[19] V.L.V. Granado, Gomes, M. T. S. R., A. Rudnitskaya, Molecularly Imprinted Polymer Thin-Film Electrochemical Sensors, Methods in Molecular Biology. 2027 (2019) 151-161.

[20] I.A. Nicholls, J. Rosengren, Molecular Imprinting of Surfaces., Bioseparation. 10 (2001) 301-305.

[21] R. Pernites, R. Ponnapati, M.J. Felipe, R. Advincula, Electropolymerization molecularly imprinted polymer (E-MIP) SPR sensing of drug molecules: Pre-polymerization complexed terthiophene and carbazole electroactive monomers, Biosensors & Bioelectronics. 26 (2011) 2766-2771.

[22] R.D. Crapnell, A. Hudson, C.W. Foster, K. Eersels, B. van Grinsven, T.J. Cleij, C.E. Banks, M. Peeters, Recent Advances in Electrosynthesized Molecularly Imprinted Polymer Sensing Platforms for Bioanalyte Detection, Sensors, 19 (2019) 1204.

[23] S. El-Akaad, M.A. Mohamed, N.S. Abdelwahab, E.A. Abdelaleem, S. De Saeger, N. Beloglazova, Capacitive sensor based on molecularly imprinted polymers for detection of the insecticide imidacloprid in water, Scientific Reports. 10 (2020) 14479.

[24] N. Shaabani, N.W.C. Chan, W.E. Lee, A.B. Jemere, Electrochemical Determination of Naloxone Using Molecularly Imprinted Poly(para-phenylenediamine) Sensor, JES. 167 (2020).

[25] P.S. Sharma, A. Pietrzyk-Le, F. D'Souza, W. Kutner, Electrochemically synthesized polymers in molecular imprinting for chemical sensing, Analytical and Bioanalytical Chemistry, 402 (2012) 3177-3204.

[26] J.-. Moon, D.-. Kim, M.H. Kim, J.-. Han, D.-. Jung, Y.-. Shim, A disposable amperometric dual-sensor for the detection of hemoglobin and glycated hemoglobin in a finger prick blood sample, Biosensors & Bioelectronics. 91 (2017) 128-135.

[27] A. Witkowski, M.S. Freund, A. Brajter-Toth, Effect of electrode substrate on the morphology and selectivity of overoxidized polypyrrole films, Analytical Chemistry, 63 (1991) 622-626.

[28] C. Hsueh, A. Brajter-Toth, Electrochemical Preparation and Analytical Applications of Ultrathin Overoxidized Polypyrrole Films, Analytical Chemistry. 66 (1994) 2458-2464.

[29] H. Ge, G. Qi, E.T. Kang, K.G. Neoh, Study of overoxidized polypyrrole using X-ray photoelectron spectroscopy, Polymer, 35 (1994) 504-508.

[30] A. Ramanavičius, A. Ramanavičienė, A. Malinauskas, Electrochemical sensors based on conducting polymer—polypyrrole, Electrochimica Acta. 51 (2006) 6025-6037.

[31] A. Namvar, K. Warriner, Microbial imprinted polypyrrole/poly(3-methylthiophene) composite films for the detection of Bacillus endospores, Biosensors & Bioelectronics. 22 (2007) 2018-2024.

[32] Z. Mazouz, S. Rahali, N. Fourati, C. Zerrouki, N. Aloui, M. Seydou, N. Yaakoubi, M.M. Chehimi, A. Othmane, R. Kalfat, Highly Selective Polypyrrole MIP-Based Gravimetric and Electrochemical Sensors for Picomolar Detection of Glyphosate, Sensors, 17 (2017) 2586.

[33] B. Schweiger, J. Kim, Y.J. Kim, M. Ulbricht, Electropolymerized molecularly imprinted polypyrrole film for sensing of clofibric acid, Sensors, 15 (2015) 4870-4889.

[34] D.M. Hawkins, D. Stevenson, S.M. Reddy, Investigation of protein imprinting in hydrogel-based molecularly imprinted polymers (Hydrogels)., Analytica Chimica Acta. 542 (2005) 61-65.

[35] M.V. Sullivan, O. Clay, M.P. Moazami, J.K. Watts, N.W. Turner, Hybrid Aptamer-Molecularly Imprinted Polymer (aptaMIP) Nanoparticles from Protein Recognition-A Trypsin Model, Macromolecular Bioscience. 21 (2021) e2100002.

[36] F. Allabush, P.M. Mendes, J.H.R. Tucker, Acrylamide-dT: a polymerisable nucleoside for DNA Incorpation. , RSC Advances. 9 (2019) 31511-31511.

[37] T. Ami, K. Fujimoto, Click Chemistry as an Efficient Method for Preparing a Sensitive DNA Probe for Photochemical Ligation, Chembiochem : a European Journal of Chemical Biology. 9 (2008) 2071-2074.

[38] D.R. Kryscio, M.Q. Fleming, N.A. Peppas, Conformational studies of common protein templates in macromolecularly imprinted polymers, Biomedical Microdevice. 14 (2012) 679-687.

[39] N. Elgrishi, K.J. Rountree, B.D. McCarthy, E.S. Rountree, T.T. Eisenhart, J.L. Dempsey, A Practical Beginner's Guide to Cyclic Voltammetry, Journal of Chemical Education. 95 (2018) 197-206.

[40] F.T.C. Moreira, S. Sharma, R.A.F. Dutra, J.P.C. Noronha, A.E.G. Cass, M.G.F. Sales, Smart plastic antibody material (SPAM) tailored on disposable screen printed electrodes for protein recognition: Application to myoglobin detection, Biosensors & Bioelectronics. 45 (2013) 237-244.

[41] V.V. Shumyantseva, T.V. Bulko, I.H. Baychorov, A.I. Archakov, Molecularly imprinted polymers (MIP) in electroanalysis of proteins, Biochemistry (Moscow) Supplement Series B. 10 (2016) 145-151.

[42] H.F. El-Sharif, D. Stevenson, S.M. Reddy, MIP-based protein profiling: A method for interspecies discrimination, Sensors and Actuators. B, Chemical. 241 (2017) 33-39.

[43] M.M. Pedroso, M.V. Foguel, D.H.S. Silva, M.P.T. Sotomayor, H. Yamanaka, Electrochemical sensor for dodecyl gallate determination based on electropolymerized molecularly imprinted polymer, Sensors and Actuators. B, Chemical. 253 (2017) 180-186.

[44] O. Kimhi, H. Bianco-Peled, Study of the Interactions between Protein-Imprinted Hydrogels and Their Templates, Langmuir. 23 (2007) 6329-6335.

[45] E. Verheyen, J.P. Schillemans, M. Van Wijk, M.A. Demeniex, W.E. Hennink, C.F. Van Nostrum, Challenges for the Effective Molecular Imprinting of Proteins. Biomaterials, 32 (2011) 3008-3020.

[46] M. Zayats, A.J. Brenner, P.C. Searson, Protein Imprinting in Polyacrylamide-based gels, Biomaterials, 35 (2014) 8659-8668.

[47] A. Poma, A. Guerreiro, M.J. Whitcombe, E.V. Piletska, A.P.F. Turner, S.A. Piletsky, Solid-Phase Synthesis of Molecular Imprinted Polymer Nanoparticles with a Reusable Template - "Plastic Antibodies"., Advance Functional Materials. 23 (2013) 2821-2817.

[48] Y. Wang, Q. Zhang, Y. Ren, L. Jing, T. Wei, Molecularly Imprinted Polymer Thin Film Based Surface Plasmon Resonance Sensor to Detect Hemoglobin, Chemical Research in Chinese Universities, 30 (2014) 42-48.